

Article

The Effect of Various Contaminants on the Surface Tribological Properties of Rail and Wheel Materials: An Experimental Approach

Rabesh Kumar Singh ¹, Mahesh Shindhe ^{2,*}, Prashant Rawat ^{3,*}, Ashish Kumar Srivastava ⁴,
Gyanendra Kumar Singh ⁵, Rajesh Verma ⁶, Javed Khan Bhutto ⁶ and Hany S. Hussein ^{6,7}

¹ Centre for Advanced Studies, Lucknow 226031, Uttar Pradesh, India

² Department of Mechanical Engineering, Indian Institute of Technology (ISM), Dhanbad 826004, Jharkhand, India

³ Department of Aerospace Engineering, Indian Institute of Technology Madras, Chennai 600036, Tamil Nadu, India

⁴ Department of Mechanical Engineering, G.L. Bajaj Institute of Technology and Management, Greater Noida 201306, Uttar Pradesh, India

⁵ Department of Mechanical Engineering, School of Mechanical, Chemical and Materials Engineering, Adama Science and Technology University, Adama P.O. Box 1888, Ethiopia

⁶ Department of Electrical Engineering, College of Engineering, King Khalid University, Abha 61411, Saudi Arabia

⁷ Department of Electrical Engineering, Faculty of Engineering, Aswan University, Aswan 81528, Egypt

* Correspondence: itsshindhe@gmail.com (M.S.); prashant.rawat@iitm.ac.in (P.R.)

Abstract: This study reports on the tribological behavior of Indian rail track and wheel materials under different contaminants. A pin-on-disc tribometer was selected for the experimental analysis in ambient conditions (temperature of 24.9 °C and relative humidity of 66%). Sand, mist, leaves, and grease were the contaminants used in this investigation. The railway track was used to make the pin, and the wheel was used to make the disc. The acquired results were analyzed using frictional force and wear depth as a function of time as the variables. These pollutant effects were compared to no-contaminant conditions. It was observed that the sand increased the friction force and wear depth, whereas oil decreased friction and wear. Mist and leaves also reduced friction and wear. The effect of leaves was higher than the mist. The effect of load on various contaminants was also investigated. The results showed that as the load increased, the friction force and wear also increased for all contaminants. The results of this study can help in understanding the wear phenomenon of wheels and rail tracks in different parts of India.

Keywords: wear; rail track; rail wheels; pin-on-disc; friction; contamination



Citation: Singh, R.K.; Shindhe, M.; Rawat, P.; Srivastava, A.K.; Singh, G.K.; Verma, R.; Bhutto, J.K.; Hussein, H.S. The Effect of Various Contaminants on the Surface Tribological Properties of Rail and Wheel Materials: An Experimental Approach. *Coatings* **2023**, *13*, 560. <https://doi.org/10.3390/coatings13030560>

Academic Editor: Esteban Broitman

Received: 3 February 2023

Revised: 24 February 2023

Accepted: 1 March 2023

Published: 5 March 2023



Copyright: © 2023 by the authors. Licensee MDPI, Basel, Switzerland. This article is an open access article distributed under the terms and conditions of the Creative Commons Attribution (CC BY) license (<https://creativecommons.org/licenses/by/4.0/>).

1. Introduction

Goods and public transportations are critical for the growth of any nation. Because of its low cost, the railway is one of India's most vital modes of transportation. The maintenance of railway tracks and wheels is difficult and necessary because both are directly exposed to different environmental conditions. As the rail moves from one region to another, the environmental conditions may change gradually or drastically. This change in environmental conditions profoundly influences the wear and friction behavior of the wheel and track. Further, the railway tracks are also surrounded by unwanted objects or pollutants, which may get engaged between the railway wheels and tracks. These pollutants also affect the wear and friction between the railway track and the wheel. These pollutants include small plants around the rail track or left-out grease after the maintenance of the railway tracks also affect the wear and friction behavior between the railway track and wheel.

Under these environmental conditions, it is critical to monitor the wear of rail tracks and wheels [1]. If the wear on the rail track and wheels is not noticed and resolved promptly, it can lead to fatal accidents. Hence, it is essential to properly investigate the tribological characteristics of rail tracks and wheels and their performance under varied pollutants, similar to real-life situations. Wheel and rail tracks perform motion in two ways, i.e., rolling and sliding (Figure 1). The wheel flange and rail head undergo slipping motion, whereas the rail head and wheel tread accomplish rolling motion [2]. Extreme sliding motion occurs when the wheel flange and rail head make contact. Wear and friction are high at this point of contact, and the contact area is about 1 cm^2 [3]. It is also known that friction is a desired property for the rail wheel pair, but it should not be too high or too low [4]. A desirable coefficient of friction between the rail track and wheel is 0.25 to 0.4. This range of coefficient of friction is considered to be desirable, which provides sufficient traction between the rail track and wheel to maintain control and prevent sliding. Within this range, the wear and tear between the rail track and wheel are minimal.

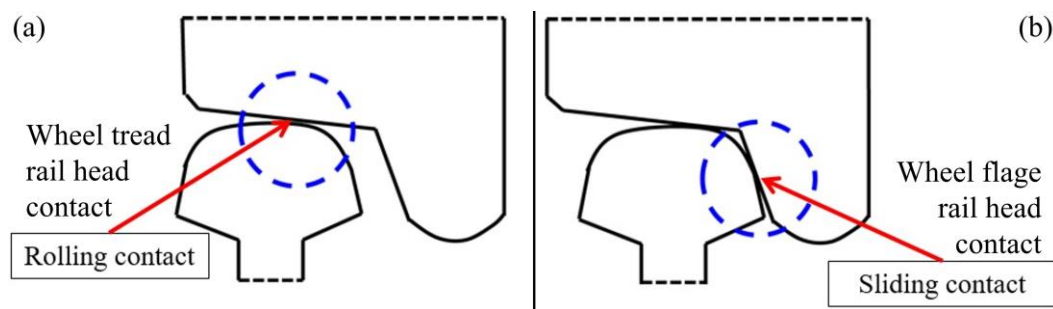


Figure 1. Rail track and wheel contact.

1.1. Effect of Temperature

Diverse external environments and pollutants affect the contact conditions and alter the tribology between the rail track and wheel. Some researchers investigated the influence of temperature variation, which takes place due to changes in bulk material characteristics [5]. As the temperature at the rail track and wheel contact increases, the oxidation process at the contact point also increases. Furthermore, the oxidation at the point the rail track and wheel meet causes wear and friction [6]. The increase in temperature contributes to the formation of oxide debris, which contributes to the formation of a wear-resistant layer, which reduces the wear [7]. Furthermore, a few studies have also shown a reduction in wear and friction levels with an increase in temperature [8,9]. However, the wear rate on contact surfaces increases significantly with the reduction in external temperature [10].

1.2. Effect of Humidity

The relative humidity reduces the coefficient of friction until saturation, at which time the coefficient of friction becomes independent of relative humidity [11]. Above 70% relative humidity, the friction levels are low, whereas the friction levels at 40% relative humidity (approximately) are comparable to dry circumstances [12]. Corrosive wear in train wheels is more prevalent when relative humidity exceeds 80%. If the relative humidity is greater than 10% but less than 70%, adhesive wear occurs [13]. An increase in humidity causes an oxide layer to grow on the worn surface. As a result, it reduces the adhesion phenomena, lowering the coefficient of friction [14]. Along with the presence of water, the parameters between the points of contact change. Water is known to diminish the adhesion of the rail to the wheel. For flat surfaces, the adhesion coefficient attained is low due to the presence of water. Surface oxidation is responsible for this phenomenon. This decrease in adhesion is influenced by surface topography, water temperature, and surface oxidation [15]. The water temperature also has a significant effect on adhesion. Adhesion increases if the temperature is kept high under wet environmental conditions [16]. If snow particles are present in the contact, they melt in layers responding to pressure. This results

in the formation of haematite (Fe_2O_3) flakes. This phenomenon reduces both friction and wear. The principal mechanism of wear is oxidative wear due to the presence of snow [17]. The hardness of hematite flakes is greater than the rail track and wheel. These flakes are also brittle and can be crushed easily into particles of small sizes during sliding. This hard particle debris between the rail track and wheel then acts as third-body wear debris [18]. These oxide flakes undergo minimal elastic and/or plastic deformation during contact. Furthermore, as the hardness of these particles is greater than the rail track and wheel, they embed themselves into the clean area of the rail track and wheel. These embedded flakes now act as a barrier between the rail track and wheel, which avoids direct contact between the rail track and wheel [19]. Moreover, the embedded flake particles help in holding the applied lubricants more firmly for a longer time. As a result, the wear rate between the rail track and wheel reduces.

1.3. Effect of Lubricant

Lubricants are designed to reduce friction wherever they are employed [20,21]. When a lubricant is applied between the rail wheel pair, the coefficient of friction decreases. Grease, as a lubricant, performs a similar function and prevents subsurface degradation [22]. In dry contact conditions (without lubricant), surface damage occurs [23]. Furthermore, when oil and water are added simultaneously, they generate a boundary or mixed film that reduces adhesion between the rail and the wheel [24]. Compared to dry circumstances, the presence of leaves effectively lowers the coefficient of friction by a factor of four. The leaves cause a slick coating to grow on the tracks [25]. Leaves also have a chemically reactive surface. This chemically reactive surface of phosphate and calcium is easily sheared away [26]. If the glycol water combination is present and leaves are added, the coefficient of friction does not reduce. In this scenario, the glycol water combination hinders the activity of leaves [27].

1.4. Effect of Parameters

Several other impurities, such as cement and iron oxides, affect the friction and wear between the rail track and wheel. Silica granules in cement penetrate rail wheel contact and cause three-body abrasion, in the same way as sand. Cement also reduces the energy wear coefficient [28]. Oxide flakes lower the amount of wear. When oxide layers are thin, they protect against wear and smooth topography. However, thicker layers or rough topography increase the wear [9,28]. The iron oxide can assist in the preservation of friction values. There is a relationship between increasing wear volume and acting pressure [27,29]. The wear rate depends on contact pressure; as the contact area increases, the wear rate decreases because the contact pressure decreases. As a result, independent of load, the wear rate increases as contact pressure increases [30]. High adhesive force is related to high frictional force [31]. The frictional force defines the grip between the rail track and the wheel. This is defined as the degree of traction or traction level. It is referred to as the amount of grip or friction between two surfaces in contact with each other. The degree of traction is also affected by these various parameters. If the degree of traction is high, then there is better control and stability, whereas lower levels of traction can increase the risk of sliding, slipping, or losing control. The traction level increases in the presence of leaves or water, which is equivalent to the absence of leaves [32].

The above review proved that various environmental variables substantially impact the wear phenomena of rail wheels and tracks. The rail tracks are open environments surrounded by dirt and contaminants. A train might encounter these multiple adversaries in a single run. The current investigation addressed the effect of contaminants found around the rail track on the wear rate of the rail track and wheel. The experiment was conducted using a universal pin-on-disc tribometer. The rail track was used to make the pin, and the rail wheel was used to make the disc. The contaminants considered for the study were sand particles, leaves, mist, and grease. All the contaminants were collected from the nearest railway track. The effect of these contaminants on the wear rate between the rail track and wheel was examined and compared with the pure dry (no contamination)

situation. This investigation was conducted at room temperature and relative humidity for three different loading conditions 5 N, 10 N, and 15 N.

2. Materials and Experiment

2.1. Experimental Setup

A pin-on-disc tribometer (DUCOM) was used in the experiment (Figure 2). The setup consisted of three components: a tester with a pin and disc configuration, a controller for managing rpm, temperature, and time, and a computer system for data storage and analysis. The load capability of the machine used as a tribometer was 5–100 N. The disc had a rotational speed minimum of 200 and a maximum of 2000. The machine had several environments to perform different tests. The pin was static in a pin holder, and the disc rotated according to the input value within the machine's capacity. The track diameter was adjustable. Figure 2c depicts the configuration for forming mist using a minimum quantity lubricant (MQL) unit and compressor, as well as a nozzle at the pin and disc arrangement. The temperature sensor in Figure 2c displays the room temperature and humidity.

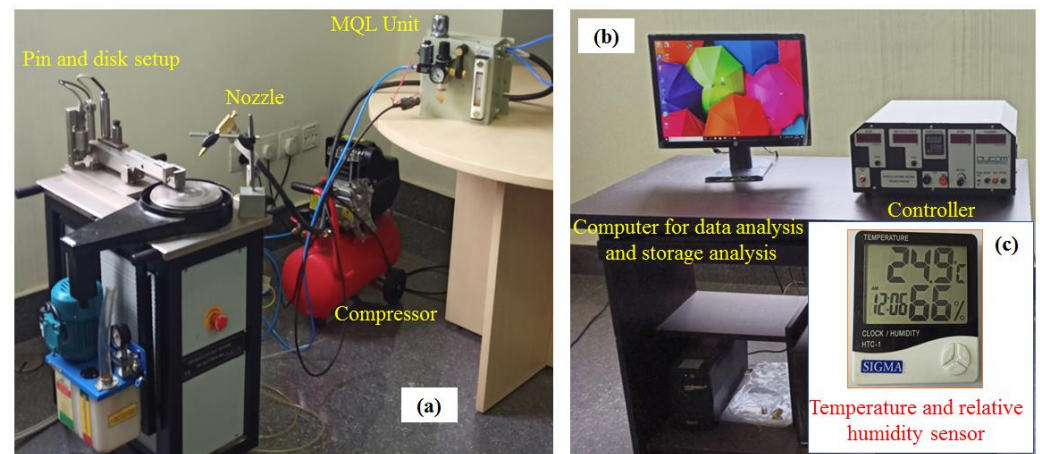


Figure 2. (a) Pin-on-disc tribometer setup, (b) Control and data analysis system, and (c) Temperature and relative humidity sensor showing the ambient conditions.

2.2. Materials

The Research Design and Standards Organisation (RDSO), Lucknow, India, provided the experimental materials, i.e., both railway track and wheel. The chemical composition and mechanical properties of the materials are shown in Tables 1–4. Figure 3 shows the preparation of a test specimen of a pin made of rail material and a disc built of wheel material. Both were prepared as per the ASTM G99 testing standard. The peak diameter of the disc (rail wheel) was 155 mm with 8 mm disc thickness. The surface roughness of the disc before the experiment was 0.2 μm .

Table 1. Chemical components in the wheel [33].

Specification	C %	Mn %	P %	S %	Si %
IRS: R19/93	0.52	0.60–0.85	0.03	0.03	0.15–0.4

Table 2. Mechanical properties of wheel [33].

Specification	Yield Strength (MPa)	Ultimate Tensile Strength (MPa)
IRS: R19/93	50% of Ultimate tensile strength	820–940

Table 3. Chemical components in rail [33].

Specification	C %	Mn %	P %	S %	Si %	Al %
Rail (grade 880)	0.60–0.80	0.80–1.35	0.03	0.03	0.10–0.50	0.015

Table 4. Mechanical properties of rail [33].

Specification	Yield Strength (MPa)	Ultimate Tensile Strength (MPa)
Rail (grade 880)	460	880

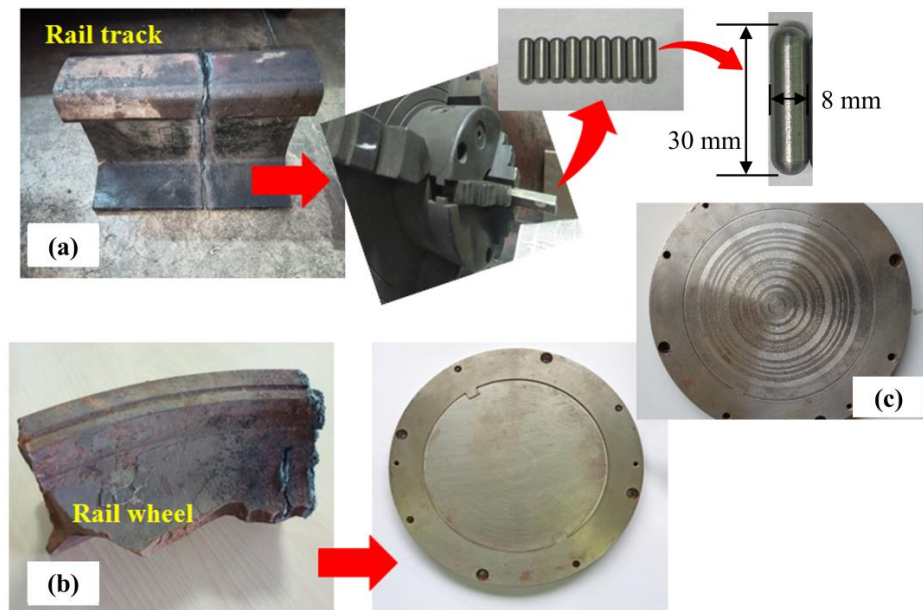


Figure 3. Fabrication of (a) pin and (b) disc from rail track and wheel material, (c) Disc after testing.

2.3. Experimental Details

The experiment was carried out under five distinct conditions. There were three experiments for each condition with three distinct loads, namely 5 N, 10 N, and 15 N. Table 5 displays the experimental details. The initial contact Hertzian pressure was calculated using the Hertzian contact theory equation (Equation (1)). The theory makes the following assumptions: (i) Contacting bodies are elastic, (ii) Material properties of both contacting bodies are Homogeneous and isotropic, and (iii) Deformation is small.

$$Initial\ Contact\ Hertzian\ Pressure\ (P_0) = F \times \left[\frac{1 - \nu^2}{E_{eff}} \right] \times \left[(R_{pin}^{-1.5} + R_{disc}^{-1.5})^2 \right] \quad (1)$$

where,

P_0 is the initial contact Hertzian pressure in Mpa,

F is the applied normal load in N (5 N, 10 N, and 15 N for this investigation),

ν is the Poisson’s ratio of the pin and disc,

E_{eff} is the effective elastic modulus of the contacting bodies in Pa^{-1} ,

R_{pin} is the radius of curvature of the hemispherical nose of the cylindrical pin in mm,

R_{disc} is the radius of the curvature of the flat disc in mm.

Here, the E_{eff} can be calculated using Equation (2).

$$\frac{1}{E_{eff}} = \frac{1 - \nu_{pin}^2}{E_{pin}} + \frac{1 - \nu_{disc}^2}{E_{disc}} \quad (2)$$

where,

ν_{pin} is the Poisson's ratio of pin (0.3 for this investigation),

ν_{disc} is the Poisson's ratio of the disc (0.3 for this investigation),

E_{pin} is Young's modulus of the pin in GPa (190 GPa for this investigation),

E_{disc} is Young's modulus of the disc in GPa (200 GPa for this investigation).

Here, the radius of curvature of the pin can be calculated using Equation (3).

$$R_{pin} = \frac{(h - r_{nose})^2}{2 \times r_{nose}} \quad (3)$$

where,

h is the total height of the pin in mm (30 mm for this investigation),

r is the radius of the hemispherical nose in mm (4 mm for this investigation).

Here, the radius of curvature of the flat disc can be estimated using Equation (4).

$$R_{disc} = \frac{D^2}{8t} \quad (4)$$

where,

D is the diameter of the disc in mm (155 mm for this investigation),

t is the thickness of the disc in mm (8 mm for this investigation).

The initial contact Hertzian pressure for loading conditions 5 N, 10 N, and 15 N can be estimated using Equations (1)–(4). The estimated initial contact Hertzian pressure for loading conditions 5 N, 10 N, and 15 N were 3.62 MPa, 7.25 MPa, and 10.88 MPa, respectively.

According to the Track Design Handbook for Broad Gauge, published by the Research Designs and Standards Organization (RDSO), the maximum permissible contact pressure between the wheel and the track is 10–12 MPa for passenger trains and 14–16 MPa for heavy freight trains. The experimental initial contact Hertzian pressure values approximately reached the maximum standard values provided by the RDSO at higher loads only.

Table 5. Experimental details.

Parameters	Dry
Temperature (°C)	24.9
Relative Humidity (%)	66
Load (N)	5, 10, 15
Sliding Distance (m)	100
Time (s)	100
sliding velocity (m/s)	1

The experiment was carried out over a 100 m continuous sliding distance. The sliding speed was also maintained at 1 m/s. The temperature was 24.9°C, and the relative humidity was 66%, which remained constant throughout the experiment. There were five conditions dry, using water as MQL, sand, leaf, and grease. The wear track diameter and the rpm are shown in Table 6. The variation of wear track diameter was done by keeping the sliding velocity constant.

Table 6. Wear track diameter, RPM variation as per the different loads.

Conditions	Variables	5 N	10 N	15 N
Dry	Track diameter (mm)	15	22	40
	RPM	1273	868	477
Leaves	Track diameter (mm)	48	54	60
	RPM	398	354	318
Sand	Track diameter (mm)	72	76	82
	RPM	265	251	239
MQL	Track diameter (mm)	94	90	88
	RPM	212	212	217
Grease	Track diameter (mm)	96	104	108
	RPM	199	184	174

The MQL represented the mist conditions of the Western Ghats or during rainfall. The mist would probably affect the tribology of the rail and wheel. The water in MQL was supplied at a rate of 200 mL/hr to create a mist condition for the pin-on-disc test. Babool (*Acacia Nilotica*) leaves were used. These leaves are widely available in India. Furthermore, these plants are frequently seen near railway lines. As a result, these leaves will get in between the rail and wheel contacts, influencing the tribology between the rail and wheel. The effect of these leaves on the contact state of the rail wheel was measured using the leaves in a pin-on-disc tribometer configuration. The leaves and sand used for the experiments can be seen in Figure 4a,b. The sand was fairly common in the Rajasthan state since there is a desert area (Thar Desert), and several rivers across the Indian continent carry the sand. Sand might become entrapped between the rail and the wheel of a railway operating in these places. The sand was applied between the rail and the wheel to achieve the necessary amount of adhesion when adhesion declined. As a result, it became vital to investigate the influence of sand on rail and wheel tribology. The sand used in the study was river sand obtained from the riverbanks. Another condition in the current investigation was the influence of lubrication or grease. Grease and lubricants were placed on the railway lines when appropriate. As a result, grease might have easily gotten between the rail and wheel contact. As a result, the current work considered the effect of grease by inserting grease between the pin and disc. Figure 4c depicts the grease utilized. Table 7 displays the grease specifications.

All four conditions, namely, leaves, sand, MQL, and grease, were compared with the fifth condition, which was the pure dry condition. The dry condition had ambient humidity and ambient temperature, and no contaminants. Here, all experiments were carried out at 24.9°C and 66% relative humidity.



Figure 4. The contaminating materials considered for the experimental work (a) Babool Leaves (*Acacia Nilotica*), (b) Sand, and (c) Grease.

Table 7. Grease Specification [34].

Name	Method	Units	Grease Specification
Thickener	-	-	Lithium
Base Oil	-	-	Mineral Oil
Appearance	BAM 300	-	Bright and shiny
Structure	-	-	Smooth and buttery
NLGI Grade	ASTM D 217	-	3
Dropping Point	IP 132	°C	192
Cone Penetration (60 strokes)	IP 50	10 ths/mm	231
Base Oil Viscosity (at 100 °C)	IP 71	cSt	15.4
4 Ball Weld Point	IP 239	kg	200

3. Results and Discussion

The friction force vs. time and wear depth vs. time graph were obtained from experiments performed on a pin-on-disc tribometer in five distinct situations. Each condition was subjected to three experiments with three distinct loads (5 N, 10 N, and 15 N).

3.1. Friction Force

Figure 5 shows the fluctuation of friction force vs. time at three weights. The graph clearly shows that the sand had the greatest friction levels. The grease condition offered the lowest values of friction force. Compared to the dry conditions, oil reduced friction by a factor of 8. Only the sand had a higher friction level compared to the dry conditions. The friction levels were relatively lower in the other conditions. When *Acacia Nilotica* leaves were present between the rail and the wheel, the friction levels were lower than in the dry state but higher than in the grease condition. The friction levels in the mist state, measured by MQL, were lower than in the dry condition but higher than in the *Acacia Nilotica* leaves.

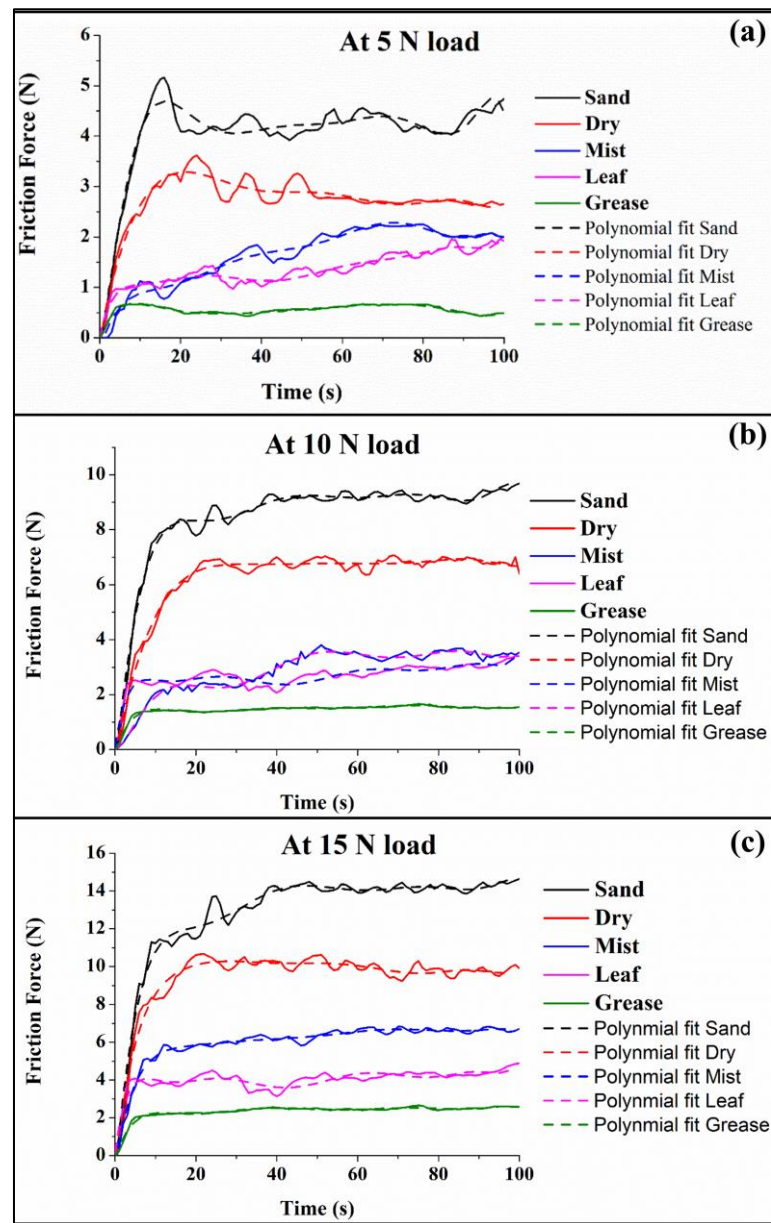


Figure 5. Variation of friction force versus time for normal loads (a) 5 N (b) 10 N (c) 15 N.

In each case, first, the friction force grew rapidly until a certain point, after which it stabilized but exhibited occasional variations with no net increase in friction force. Except for the grease condition, the curvature of each condition varied. The oil made the slide smooth, resulting in little to no fluctuations. The stick-slip phenomenon caused the variations [35].

3.2. Wear Depth

Figure 6 illustrates the wear depth vs. time at three loads for all five conditions at a fixed load of 5 N. The graph shows that the wear was growing across the graph under all conditions. Sand caused the highest wear compared to the other conditions. The grease resulted in the least amount of wear. Compared to the dry environment, the mist condition had much less wear. The *Acacia Nilotica* leaves have reduced wear even more than the mist condition.

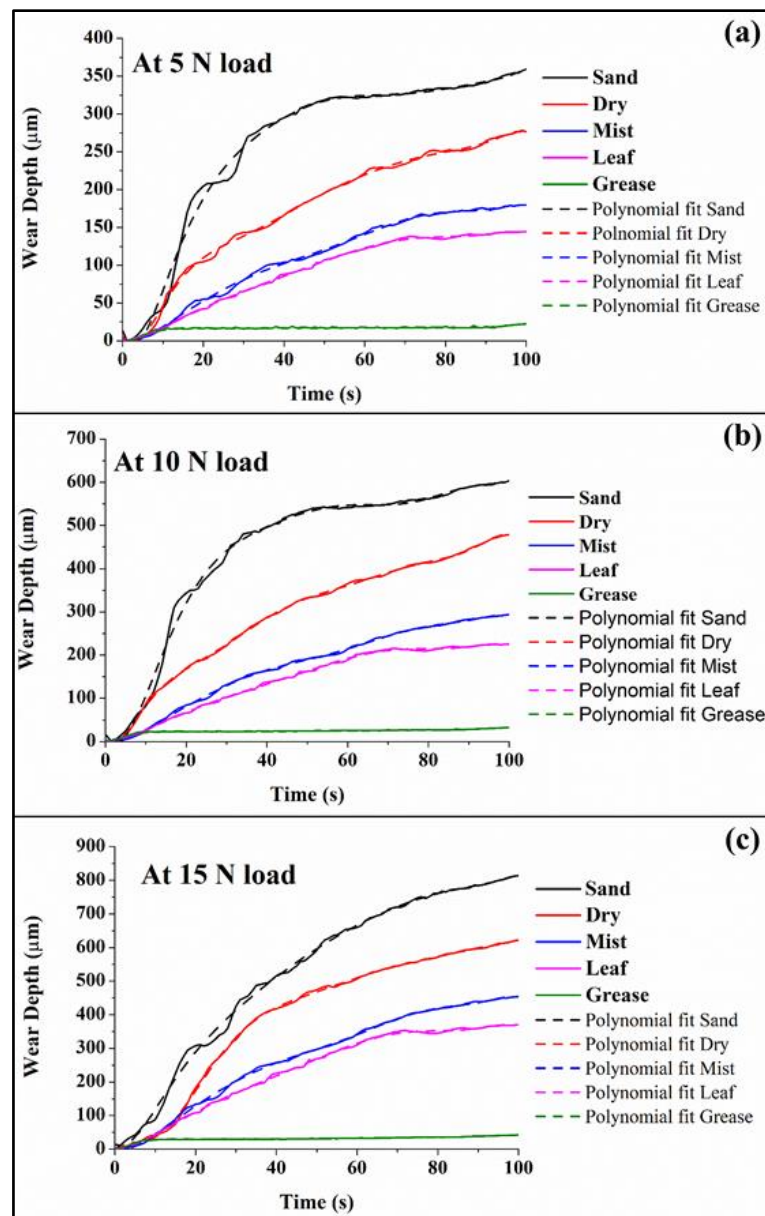


Figure 6. Variation of wear depth versus time for normal loads (a) 5 N (b) 10 N (c) 15 N.

The curves for all circumstances increased, but not significantly, except for the sand condition, where the rise was significant. For the first 10 s, the dry, leaf, mist, and grease behaviors overlapped. The slope was highest in the sand condition and reduced in the following order: dry, mist, *Acacia Nilotica* leaves, and grease. For all situations, the slope steadily diminished. The slope for the grease condition was insignificant. Wear increased as load increased. The slope was steeper at first but gradually decreased in each case. Initially, the dry and sand condition curves overlapped. Also, the curves for mist and leaf conditions overlapped for a few seconds before they separated. The grease had some slope initially, but the slope diminished as the curve progressed.

3.3. Effect of Load on Friction Force

Figure 7 illustrates the friction force as a function of time under all situations. The amount of friction force increased significantly with increasing loads in the sand condition, as shown in Figure 7a. In contrast, the behavior was similar at all three friction loads. The friction force curve fluctuated less at 5 N and more at 15 N. In the dry situation,

increasing the load caused high friction levels, as seen in Figure 7b. The curve's behavior was consistent for all loads. At smaller loads, the friction force fluctuated less. Figure 7c shows that for the mist conditions, larger loads resulted in increased wear and friction force. The friction force increased with increasing load (Figure 7d). The friction force curve was quite similar at all loads. Initially, there were three clear, distinct curves with little to no overlapping in the leaf state. Figure 7e for the grease condition shows that increasing the load caused a rise in the friction force. The curve at each load was different, and there was no overlapping at first. As a result, it was clear that the friction force increased due to the increase in load.

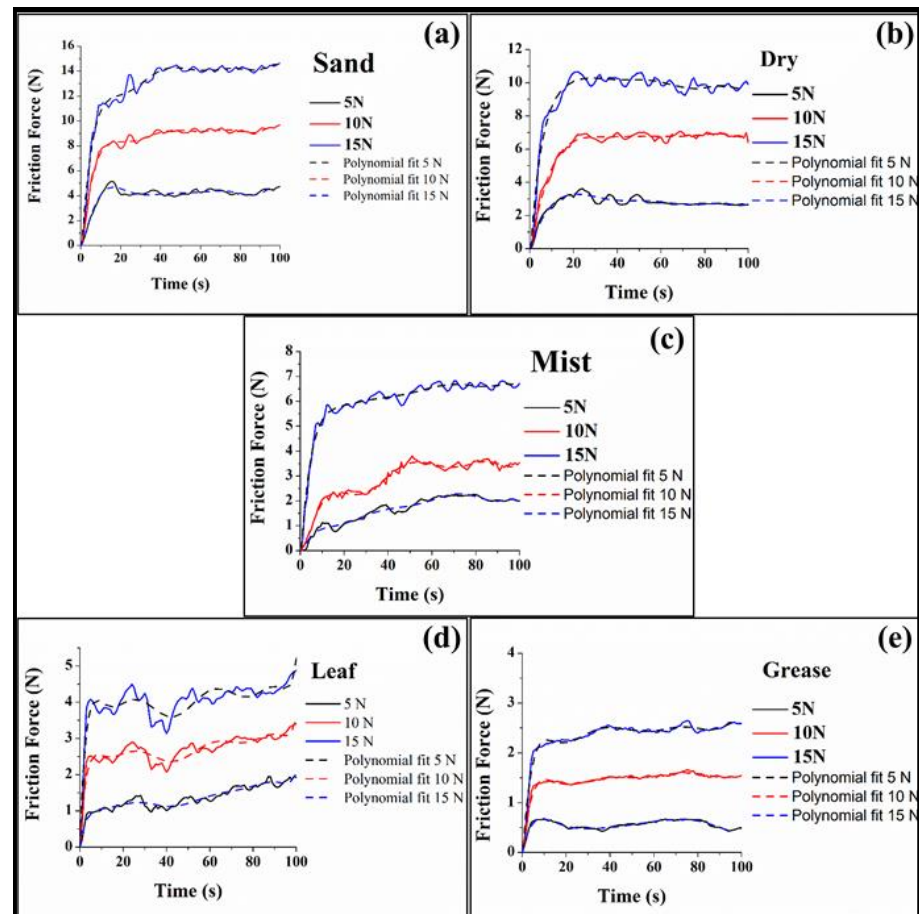


Figure 7. Effect of load on friction force for (a) sand, (b) dry, (c) mist, (d) leaf, and (e) grease.

3.4. Effect of Load on Wear Depth

Figure 8 represents the wear vs. friction force for all evaluated situations. Figure 8a shows that wear was high for larger loads in the sand condition. At first, there was significant overlap for the 10 N and 15 N loads, but the curves subsequently distinguished themselves. The wear behavior vs. time for the dry state at three different loads is given in Figure 8b. It was evident that under the dry state, an increase in load would result in excessive wear. The curve's behavior was more or less consistent for all wear loads. In dry conditions, the wear appeared to be proportional to the increase in load.

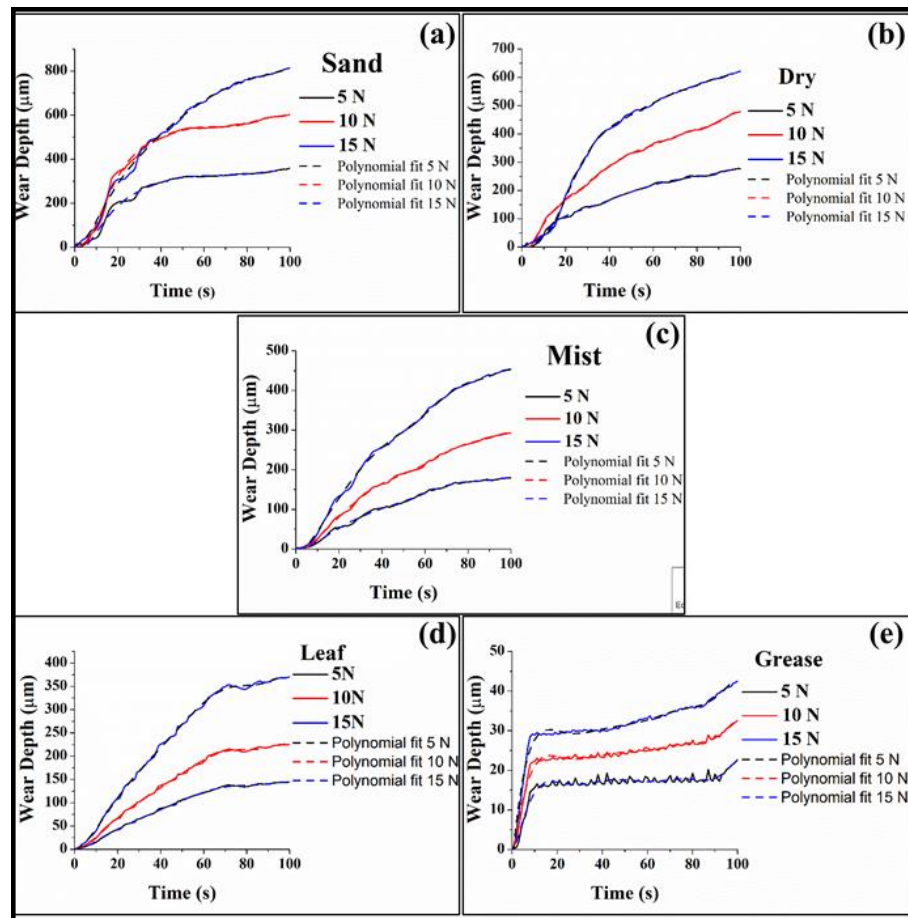


Figure 8. Effect of load on wear depth for (a) sand, (b) dry, (c) mist, (d) leaf, and (e) grease.

Figure 8c indicates that wear was higher in the mist conditions for larger loads. The 15 N load wore the most. The graph trend is consistent across all loads. For all three loads, the wear behavior was symmetrical. In this case, the increase in wear also appeared to be proportional to the increase in load for the leaf condition, as indicated in Figure 8d. Figure 8e shows that the wear depth increased with increasing load in the grease condition. The wear rose as the load increased. The wear behavior with variable load was comparable to that of other circumstances. Higher loads resulted in increased wear. The wear curve was quite similar at all loads. Initially, there was a clear distinction between the three curves with little to no overlapping for the leaf condition. In this situation, the increase in wear was proportional to the increase in load. As applied loads were increased, wear and friction were also improved. Except for the sand condition, the increase in wear was proportionate to the increase in load.

4. Conclusions

The major objective of this research was to investigate the tribological behavior of rails and wheels in a variety of situations. The investigation was done in sand, dry mist, leaf (*Acacia Nilotica*), and grease environments. For each condition, the studies were carried out at three distinct loads: 5 N, 10 N, and 15 N. The tests were carried out in a room with a temperature of 24.9°C and relative humidity of 66%. The following conclusions were obtained when compared to the dry condition:

- Both contaminants and load affected the wear rate, frictional levels, and wear depth of the rail track and wheel

- Among all the contaminants, the grease showed the least frictional levels, followed by leaves, mist, dry, and sand, irrespective of the load. However, these frictional levels increased as the load increased for all the contaminants.
- The wear depth increased with the increase in load for all the contaminants. Among all the contaminants, the highest wear depth was observed for sand contaminants, followed by dry, mist, leaves, and grease.
- The fluctuations in the frictional force increased with the increase in load for all the contaminants. The frictional forces were highest for sand conditions followed by dry, mist, leaves, and grease.
- It can be summarised that contaminants such as leaves and mist around the rail track are rather more desirable than leaving the rail track dry. However, the contaminant sand around the rail track is not desirable.

For future studies, it is advisable to apply lubricant or grease to prevent wear where excessive sliding takes place but not when rolling occurs, resulting in a loss of needed adhesion. Further study might be conducted to determine the function of particle emission from the occurring contact and the role of surface roughness in these varied rail wheel contact scenarios.

Author Contributions: Writing, R.K.S.; methodology, M.S.; conceptualization; P.R.; review and editing, software, A.K.S.; Supervision; G.K.S.; project administration, R.V.; funding acquisition, Visualization, J.K.B.; project administration, funding acquisition, H.S.H. All authors have read and agreed to the published version of the manuscript.

Funding: The authors extend their appreciation to the Deanship of Scientific Research at King Khalid University, Kingdom of Saudi Arabia, for funding this work through the Large Groups Project under Grant Number: RGP. 2/162/43.

Institutional Review Board Statement: Not applicable.

Informed Consent Statement: Not applicable.

Data Availability Statement: Not applicable.

Acknowledgments: The authors extend their appreciation to the Deanship of Scientific Research at King Khalid University, Kingdom of Saudi Arabia, for funding this work through the Large Groups Project under Grant Number: RGP. 2/162/43.

Conflicts of Interest: The authors declare no conflict of interest.

References

1. Gershon, R.R.M.; Qureshi, K.A.; Barrera, M.A.; Erwin, M.J.; Goldsmith, F. Health and Safety Hazards Associated with Subways: A Review. *J. Urban Health* **2005**, *82*, 10–20. [[CrossRef](#)]
2. Khalladi, A.; Elleuch, K. Tribological Behavior of Wheel-Rail Contact under Different Contaminants Using Pin-On-Disk Methodology. *J. Tribol.* **2017**, *139*, 011102. [[CrossRef](#)]
3. Olofsson, U.; Lewis, R.; Harmon, M. Tribology of the Wheel-Rail Contact. In *Handbook of Railway Vehicle Dynamics*; CRC Press: Boca Raton, FL, USA, 2019; pp. 281–305. ISBN 042946939X.
4. Olofsson, U.; Lyu, Y. Open System Tribology in the Wheel-Rail Contact-A Literature Review. *Appl. Mech. Rev.* **2017**, *69*, 060802. [[CrossRef](#)]
5. Bosomworth, C.; Spiriyagin, M.; Alahakoon, S.; Cole, C.; Sneath, B.; Makin, B. Rail Temperature Variation under Heavy Haul Operations. *Railw. Eng. Sci.* **2022**, *30*, 148–161. [[CrossRef](#)]
6. Blau, P.J. Elevated-Temperature Tribology of Metallic Materials. *Tribol. Int.* **2010**, *43*, 1203–1208. [[CrossRef](#)]
7. Stott, F.H. High-Temperature Sliding Wear of Metals. *Tribol. Int.* **2002**, *35*, 489–495. [[CrossRef](#)]
8. Yadav, A.; Sachin; Dubey, V.; Singh, R.K.; Sharma, A.K. Effect of Temperature and Humidity on Tribological Properties of Rail and Wheel Using Pin-On-Disc. In *Recent Advances in Smart Manufacturing and Materials: Select Proceedings of ICEM 2020*; Lecture Notes in Mechanical Engineering; Springer: Cham, Switzerland, 2021; pp. 237–244.
9. Lyu, Y.; Zhu, Y.; Olofsson, U. Wear between Wheel and Rail: A Pin-on-Disc Study of Environmental Conditions and Iron Oxides. *Wear* **2015**, *328–329*, 277–285. [[CrossRef](#)]
10. Ma, L.; Shi, L.B.; Guo, J.; Liu, Q.Y.; Wang, W.J. On the Wear and Damage Characteristics of Rail Material under Low Temperature Environment Condition. *Wear* **2018**, *394–395*, 149–158. [[CrossRef](#)]

11. Zhu, Y.; Olofsson, U.; Chen, H. Friction between Wheel and Rail: A Pin-on-Disk Study of Environmental Conditions and Iron Oxides. *Tribol. Lett.* **2013**, *52*, 327–339. [[CrossRef](#)]
12. Lewis, S.R.; Lewis, R.; Olofsson, U.; Eadie, D.T.; Cotter, J.; Lu, X. Effect of Humidity, Temperature and Railhead Contamination on the Performance of Friction Modifiers: Pin-on-Disk Study. *Proc. Inst. Mech. Eng. Part F J. Rail Rapid Transit* **2013**, *227*, 115–127. [[CrossRef](#)]
13. Barthel, A.J.; Gregory, M.D.; Kim, S.H. Humidity Effects on Friction and Wear between Dissimilar Metals. *Tribol. Lett.* **2012**, *48*, 305–313. [[CrossRef](#)]
14. Chen, Z.; He, X.; Xiao, C.; Kim, S.H. Effect of Humidity on Friction and Wear—A Critical Review. *Lubricants* **2018**, *6*, 74. [[CrossRef](#)]
15. Zhu, Y. Adhesion in the Wheel–Rail Contact. Ph.D. Thesis, Royal Institute of Technology, Stockholm, Sweden, 2013.
16. Chen, H.; Ban, T.; Ishida, M.; Nakahara, T. Experimental Investigation of Influential Factors on Adhesion between Wheel and Rail under Wet Conditions. *Wear* **2008**, *265*, 1504–1511. [[CrossRef](#)]
17. Lyu, Y.; Bergseth, E.; Olofsson, U. Open System Tribology and Influence of Weather Condition. *Sci. Rep.* **2016**, *6*, 32455. [[CrossRef](#)] [[PubMed](#)]
18. Berthier, Y.; Descartes, S.; Busquet, M.; Niccolini, E.; Desrayaud, C.; Baillet, L.; Baietto-Dubourg, M.C. The Role and Effects of the Third Body in the Wheel–Rail Interaction. *Fatigue Fract. Eng. Mater. Struct.* **2004**, *27*, 423–436. [[CrossRef](#)]
19. Kaliyannan, G.V.; Kumar, P.S.; Kumar, S.M.; Deivasigamani, R.; Rajasekar, R. Mechanical and Tribological Behavior of SiC and Fly Ash Reinforced Al 7075 Composites Compared to SAE 65 Bronze. *Mater. Test.* **2018**, *60*, 1225–1231. [[CrossRef](#)]
20. Li, C.; Li, X.; Huang, S.; Li, L.; Zhang, F. Ultra-Precision Grinding of Gd₃Ga₅O₁₂ Crystals with Graphene Oxide Coolant: Material Deformation Mechanism and Performance Evaluation. *J. Manuf. Process.* **2021**, *61*, 417–427. [[CrossRef](#)]
21. Li, C.; Piao, Y.; Meng, B.; Hu, Y.; Li, L.; Zhang, F. Phase Transition and Plastic Deformation Mechanisms Induced by Self-Rotating Grinding of GaN Single Crystals. *Int. J. Mach. Tools Manuf.* **2022**, *172*, 103827. [[CrossRef](#)]
22. Hardwick, C.; Lewis, R.; Eadie, D.T. Wheel and Rail Wear—Understanding the Effects of Water and Grease. *Wear* **2014**, *314*, 198–204. [[CrossRef](#)]
23. Vo, K.D.; Tieu, A.K.; Zhu, H.T.; Kosasih, P.B. A Tool to Estimate the Wheel/Rail Contact and Temperature Rising under Dry, Wet and Oily Conditions. In *Computers in Railways XIV: Railway Engineering Design and Optimization*; WIT Press: Billerica, MA, USA, 2014; Volume 135, pp. 191–201.
24. Olofsson, U.; Zhu, Y.; Abbasi, S.; Lewis, R.; Lewis, S. Tribology of the Wheel–Rail Contact—Aspects of Wear, Particle Emission and Adhesion. *Veh. Syst. Dyn.* **2013**, *51*, 1091–1120. [[CrossRef](#)]
25. Olofsson, U.; Sundvall, K. Influence of Leaf, Humidity and Applied Lubrication on Friction in the Wheel–Rail Contact: Pin-on-Disk Experiments. *Proc. Inst. Mech. Eng. Part F J. Rail Rapid Transit* **2004**, *218*, 235–242. [[CrossRef](#)]
26. Olofsson, U. A Multi-Layer Model of Low Adhesion between Railway Wheel and Rail. *Proc. Inst. Mech. Eng. Part F J. Rail Rapid Transit* **2007**, *221*, 385–389. [[CrossRef](#)]
27. Zhu, Y.; Lyu, Y.; Olofsson, U. Mapping the Friction between Railway Wheels and Rails Focusing on Environmental Conditions. *Wear* **2015**, *324–325*, 122–128. [[CrossRef](#)]
28. Zhu, Y.; Chen, X.; Wang, W.; Yang, H. A Study on Iron Oxides and Surface Roughness in Dry and Wet Wheel–Rail Contacts. *Wear* **2015**, *328–329*, 241–248. [[CrossRef](#)]
29. Deters, L.; Proksch, M. Friction and wear testing of rail and wheel material. *Wear* **2005**, *258*, 981–991. [[CrossRef](#)]
30. Ravikiran, A.; Jahanmir, S. Effect of Contact Pressure and Load on Wear of Alumina. *Wear* **2001**, *250–251*, 980–984. [[CrossRef](#)]
31. Mcfarlane, J.S.; Tabor, D. Relation between Friction and Adhesion. *Proc. R. Soc. Lond. Ser. A Math. Phys. Sci.* **1950**, *202*, 244–253. [[CrossRef](#)]
32. Gallardo-Hernandez, E.A.; Lewis, R. Twin Disc Assessment of Wheel/Rail Adhesion. *Wear* **2008**, *265*, 1309–1316. [[CrossRef](#)]
33. Report on rail, axle, wheel sets, Steel Authority of India Ltd. Available online: <https://sail.co.in/sites/default/files/product-brochure/2020-04/Railway-Products.pdf> (accessed on 31 December 2022).
34. Shah, R.; Tung, S.; Chen, R.; Miller, R. Grease Performance Requirements and Future Perspectives for Electric and Hybrid Vehicle Applications. *Lubricants* **2021**, *9*, 40. [[CrossRef](#)]
35. Yang, Z.; Zhang, P.; Moraal, J.; Li, Z. An Experimental Study on the Effects of Friction Modifiers on Wheel–Rail Dynamic Interactions with Various Angles of Attack. *Railw. Eng. Sci.* **2022**, *30*, 360–382. [[CrossRef](#)]

Disclaimer/Publisher’s Note: The statements, opinions and data contained in all publications are solely those of the individual author(s) and contributor(s) and not of MDPI and/or the editor(s). MDPI and/or the editor(s) disclaim responsibility for any injury to people or property resulting from any ideas, methods, instructions or products referred to in the content.